The Astrophysical Journal Letters, 922:L37 (6pp), 2021 December 1 https://doi.org/10.3847/2041-8213/ac3a05

Nonperiodic Type I Be/X-Ray Binary Outbursts

Rebecca G. Martin[1] and Alessia Franchini[2]
[1] Department of Physics and Astronomy, University of Nevada, Las Vegas, 4505 South Maryland Parkway, Las Vegas, NV 89154, USA
[2] Dipartimento di Fisica "G. Occhialini", Universitá degli Studi di Milano-Bicocca, Piazza della Scienza 3, I-20126 Milano, Italy
Received 2021 October 19; revised 2021 November 12; accepted 2021 November 15; published 2021 December 1

Abstract

Type I Be/X-ray binary outbursts are driven by mass transfer from a Be star decretion disk to a neutron star companion during each orbital period. Treiber et al. recently observed nonperiodic type I outbursts in RX J0529.8–6556 that has unknown binary orbital properties. We show that nonperiodic type I outbursts may be temporarily driven in a low eccentricity binary with a disk that is inclined sufficiently to be mildly unstable to Kozai–Lidov oscillations. The inclined disk becomes eccentric and material is transferred to the neutron star at up to three locations in each orbit: when the neutron star passes the disk apastron or one of the two nodes of the disk. The timing and magnitude of each vary with the disk argument of periapsis and longitude of the ascending node that precess in opposite directions. Calculating the orbital period of the RX J0529.8–6556 system is nontrivial but we suggest it may be >300 days, longer than previous estimates.

Unified Astronomy Thesaurus concepts: Stellar accretion disks (1579); Be stars (142); Circumstellar disks (235); Neutron stars (1108); Binary stars (154); High mass x-ray binary stars (733); Massive stars (732)

1. Introduction

Be/X-ray binaries typically consist of a Be star in a binary orbit with a neutron star companion (e.g., Reig 2011; Haberl & Sturm 2016). The Be star is rapidly rotating (Slettebak 1982; Porter 1996) and a Keplerian decretion disk forms from material that is ejected from the equator (Lee et al. 1991; Pringle 1991; Hanuschik 1996). X-ray outbursts are driven when material is transferred from the Be star disk to the neutron star. Type I Be/X-ray binary outbursts are most often observed as periodic outbursts. There are at least two mechanisms for driving type I outbursts.

First, and most commonly, if the Be star and the neutron star are in an eccentric orbit, the neutron star is able to capture material close to each periastron passage (Negueruela et al. 2001; Okazaki & Negueruela 2001; Okazaki 2007). This mechanism is only dependent on there being a moderate binary eccentricity. If the disk is coplanar to the binary orbit, outbursts occur once per orbital period and close to each periastron passage. If the disk is slightly inclined, the disk undergoes retrograde nodal precession but a regular pattern of outbursts can still occur on a timescale that is slightly $<P_{\rm orb}$ (Martin et al. 2014b).[3] The outburst structure varies depending on the difference between the longitude of ascending node of the disk and the argument of periapsis for the binary orbit. The neutron star may be able to capture material once or twice per binary orbit (Okazaki et al. 2013). If the longitude of ascending node of the disk and the binary eccentricity vector are perpendicular to each other, then the neutron star captures material twice per orbit. On the other hand, if they are aligned to each other, then material is only captured once per orbit. As the disk nodally precesses the outbursts transition between these two states but in both cases the outbursts are periodic.

Second, regular outbursts can occur in circular orbit binaries if the disk becomes eccentric (Franchini & Martin 2019). There is a small class of Be/X-ray binaries that have close to circular orbits and yet show type I outbursts (Pfahl et al. 2002; Reig 2007; Cheng et al. 2014). For disks that are close to coplanar, disk eccentricity may grow through the 3:1 resonance (Lubow 1991a, 1991b, 1992). Since the disk apsidally precesses in a prograde direction, the timescale between outbursts is slightly $>P_{\rm orb}$, but constant in time (see Figure 4 in Franchini & Martin 2019). This mechanism operates for low inclination disks, $i \lesssim 20°$. Above this inclination, the disk eccentricity does not grow through this mechanism since the strength of the resonance is greatly reduced outside of the binary orbital plane.

A hydrodynamical gas disk that is highly misaligned can undergo global Kozai–Lidov (KL; Kozai 1962; Lidov 1962) oscillations where the disk inclination and eccentricity are exchanged (Martin et al. 2014b; Fu et al. 2015a, 2015b). The critical inclination required for disk KL oscillations depends sensitively on the disk aspect ratio (Lubow & Ogilvie 2017; Zanazzi & Lai 2017). During KL oscillations, the disk overflows its Roche lobe and material is transferred to the companion (Franchini et al. 2019). The more highly inclined the disk, the more eccentric the disk becomes and the more mass that is transferred. Highly eccentric disks may be the cause of type II outbursts that occur less frequently but are more luminous (Martin et al. 2014a; Martin & Franchini 2019).

Recently, Treiber et al. (2021) observed the optical light curve for the system RX J0529.8–6556 and found that the outburst period changes over time. The outbursts are nonperiodic as the predicted orbital period changes from about 149 day to 200 day over about 10 yr. Optical and X-ray outbursts are normally thought to coincide; however, with the limited X-ray data available, this does not seem to be the case. This can occur when the disk is viewed edge on and is obscuring the star (Rajoelimanana et al. 2011); however, the positive correlation between the magnitude and color indicates

[3] See Figure 4 in Martin et al. (2014b) where the small type I like outbursts at the beginning of the simulation are occurring on a timescale slightly shorter than the orbital period.

a relatively low (non-edge-on) inclination angle for RX J0529.8–6556 (see Figure 10 in Treiber et al. 2021). The variation of the outburst period and the out of phase X-ray outbursts may be caused by a misaligned disk that is undergoing nodal precession (Treiber et al. 2021).

Since the observed outbursts are nonperiodic this suggests that the binary eccentricity must be small. If the binary eccentricity was large, the outbursts would be close to periodic no matter the disk inclination. In this Letter, we suggest that there are two requirements for nonperiodic outbursts:

1. The binary eccentricity is low.
2. The disk inclination is moderate.

The inclination must be high enough for the disk to be mildly unstable to Kozai–Lidov disk oscillations to become eccentric but not too high that the disk becomes significantly eccentric and undergoes type II like outbursts. In Section 2 we show a hydrodynamic simulation of a Be star disk in a configuration that is mildly KL unstable and the disk eccentricity grows to moderate values. We show that we can broadly reproduce the observed nonperiodic outbursts and calculate an approximate orbital period. We conclude in Section 3.

2. Hydrodynamic Simulations

There are many parameters of the RX J0529.8–6556 binary system that are unknown. These include the binary inclination, eccentricity, and orbital period as well as disk parameters such as the aspect ratio and viscosity. As a result, we do not try to explore all of the parameter space to find the best-fitting model to the observed light curve. Further we do not extract the exact periodicities from the data but leave that to future work (see, for example, Feigelson et al. 2018; Caceres et al. 2019). Instead, in this section we simply consider a test case of a hydrodynamical Be star disk simulation to show the principle that nonperiodic outbursts are possible in a misaligned viscous disk model.

2.1. Simulation Setup

We use the PHANTOM smoothed particle hydrodynamics (SPH) code (Price & Federrath 2010; Price et al. 2018) to model a Be star decretion disk with a neutron star companion on a circular orbit. We use the same disk parameters as Martin et al. (2014a). The Be star has a mass of $18\,M_\odot$ and the neutron star has a mass of $1.4\,M_\odot$. The stars are modeled with sink particles. The particles that pass inside the sink radius are accreted and their mass and angular momentum are added to the sink (Bate et al. 1995). The sink radius of the Be star is $8\,R_\odot$ and the neutron star is $1\,R_\odot$. The orbit is circular and the orbital period is 24 days. We discuss how our results apply to longer orbital period binaries later.

The disk has an initial mass of $M_{\rm d} = 10^{-8}\,M_\odot$. This is small enough that it has a negligible effect on the binary orbit and we do not include self-gravity in our calculations. The material is initially distributed with surface density $\Sigma \propto R^{-1}$ between $R_{\rm in} = 8\,R_\odot$ up to $R_{\rm out} = 50\,R_\odot$ with 500,000 SPH particles. The disk is isothermal with an aspect ratio of $H/R = 0.01$ at the disk inner edge, ensuring that it is unstable to KL oscillations. The Shakura & Sunyaev (1973) α viscosity parameter is 0.3 (e.g., Jones et al. 2008; Carciofi et al. 2012; Rímulo et al. 2018). This is typical for a fully ionized disk (King et al. 2007; Martin et al. 2019). The disk viscosity is implemented with the methods described in Lodato & Price (2010) with $\alpha_{\rm AV} = 4.7$ and $\beta_{\rm AV} = 6$. The disk is resolved with mean smoothing length per scale height of $\langle h \rangle / H = 0.64$. The disk is inclined by 50° to the binary orbital plane initially. The upper row in Figure 1 shows the initial setup. In order to analyze the dynamics of the Be star disk we bin the particles into 300 bins in particle semimajor axis. Within each bin we average the properties of the individual particles.

2.2. Disk Dynamics and Outburst Locations

Figure 2 shows the evolution of the disk inclination, longitude of ascending node, eccentricity, and argument of periapsis at semimajor axes of $20\,R_\odot$ and $40\,R_\odot$ as a function of time. The disk behaves in a similar way at different radii. The disk undergoes global damped KL oscillations. The eccentricity of the disk increases but only up to a maximum of about 0.4. This is not sufficient to drive type II like outbursts but still has a significant effect on the smaller type I outbursts.

There are three possible locations where the neutron star can accrete material during each orbit and therefore three possible outburst locations. These are where the neutron star passes Ω (longitude of the ascending node of the disk), $\Omega + \pi$ (longitude of the descending node), and $\Omega + \omega$ (disk apastron). We calculate the precession timescales with $P_{\rm node} = 2\pi/\dot{\Omega}$ (nodal precession timescale) and $P_{\rm apastron} = 2\pi/(\dot{\omega} + \dot{\Omega})$ (disk apastron precession timescale). Then the timescale between consecutive passages is calculated with

$$P_{\rm burst} = P_{\rm orb}\left(1 + \frac{P_{\rm orb}}{P_{\rm prec}}\right) \tag{1}$$

(e.g., Whitehurst 1988), where $P_{\rm prec}$ is equal to $P_{\rm node}$ or $P_{\rm apastron}$ depending on the location of the outburst.

Figure 3 shows the timescale of the neutron star passing the disk longitude of ascending node (blue) and the disk apastron (black). There are two competing precessions. The nodal precession is retrograde and so the timescale between the node crossings is always slightly less then $P_{\rm orb}$ while the apsidal precession is always prograde. The time between disk apastron crossing depends on the balance between the nodal precession and the apsidal precession. Initially the disk apastron crossing timescale is shorter than the orbital period, but after about $t = 50\,P_{\rm orb}$ it becomes longer. This clearly shows that the burst timescales are different for these two locations. The number of outbursts in each orbit depends upon the argument of periapsis for the disk. If the argument of periapsis is aligned to a node of the disk ($\omega \approx 0°$ or 180°), there can be only one outburst per orbital period. If $\omega \approx \pm 90°$, there can be three outbursts per orbit. In between there may be two outbursts. Thus, a misaligned and eccentric disk can have between one and three bursts per orbit with varying magnitudes.

2.3. Accretion Rate onto the Neutron Star

Figure 4 shows the accretion rate onto the neutron star as a function of time. We do not show the early evolution before $t = 20\,P_{\rm orb}$ since initially there is little flow as the disk expands outwards. A misaligned disk has a larger tidal truncation radius than a coplanar disk (Lubow et al. 2015; Miranda & Lai 2015). The disk eccentricity grows due to the KL effect and by a time of about $20\,P_{\rm orb}$ outbursts occur once per orbital period. These outbursts are a result of the disk eccentricity and they occur when the neutron star passes close to the disk apastron. In the second row of Figure 1 we show the disk at time $t = 30\,P_{\rm orb}$.

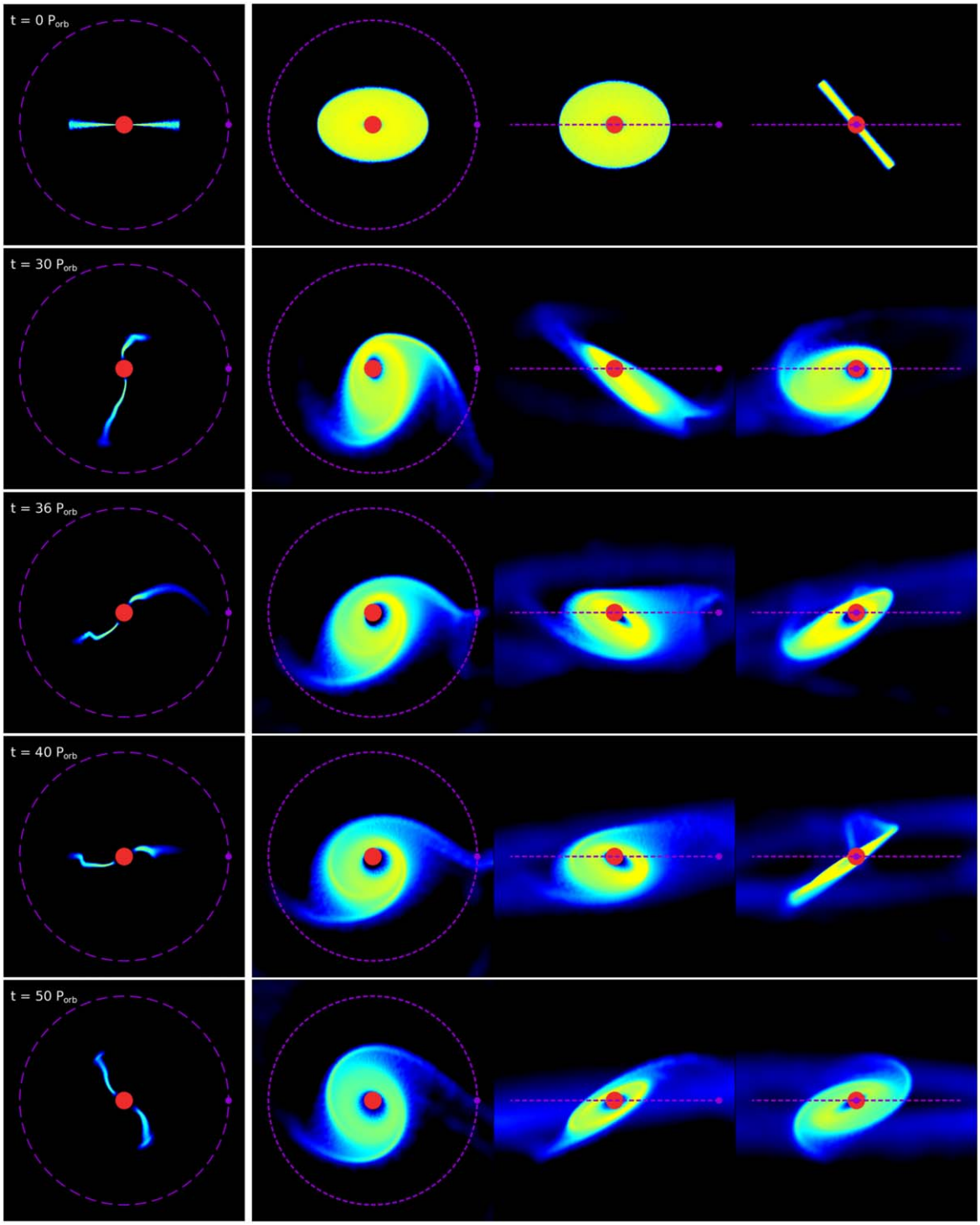

Figure 1. Disk evolution in a frame that is corotating with the binary and centered on the Be star. In each row, the left panel shows the cross section of the disk in the binary orbital plane, the x–y plane. The other three plots show the disk with a view in the x–y plane (second column), the $y-z$ plane (third column), and the x–z plane (right column). The red circles show the Be star scaled to the sink size. The magenta circle shows the neutron star (enlarged from its sink size) and the magenta dashed lines show the neutron star orbit. The times shown are $t = 0\,P_{\rm orb}$ (top), $t = 30\,P_{\rm orb}$ (second row), $t = 36\,P_{\rm orb}$ (third row), $t = 40\,P_{\rm orb}$ (fourth row), and $t = 50\,P_{\rm orb}$ (bottom row).

The cross section of the disk in the binary orbital plane (left) shows that the disk is much more extended on the lower side than the upper side and this explains why there is only one outburst per orbital period. The argument of periapsis of the disk is about 50° (at a semimajor axis of $40\,R_{\odot}$, see the blue line in the bottom row of Figure 2), this is somewhat in between the criteria for clear one or three outbursts per orbital period. However, as we can see from Figure 4, the outburst is dominated by the disk apastron passage and there is therefore only one peak. The subpeaks start to become evident at roughly $34\,P_{\rm orb}$ as the argument of periapsis moves closer to 90°. Note that at this time the two competing precessions give a similar $P_{\rm burst}/P_{\rm orb}$ (see Figure 3) and this is <1.

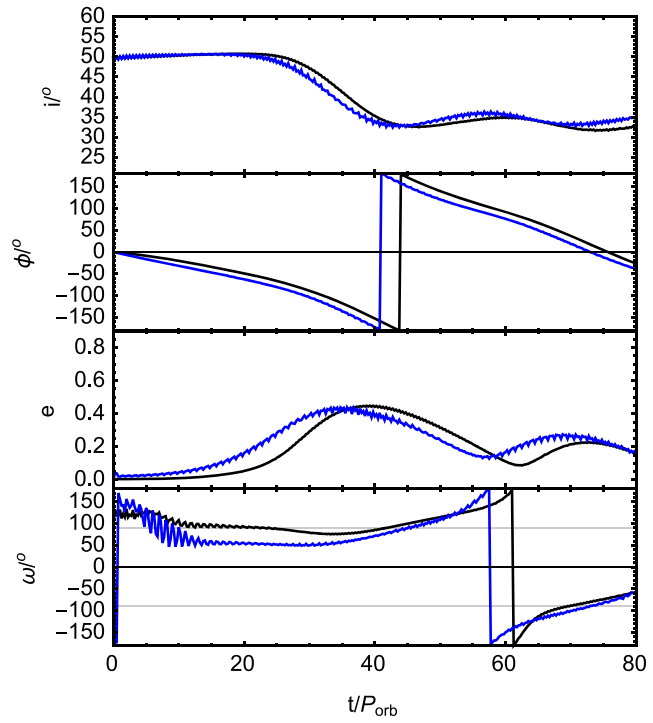

Figure 2. Evolution of the Be star disk at semimajor axes of 20 $R_\odot$ (black lines) and 40 $R_\odot$ (blue lines). The panels show the disk inclination (upper), longitude of ascending node (second), eccentricity (third), and argument of periapsis (bottom). The horizontal gray lines in the bottom panel show $\omega = \pm 90°$.

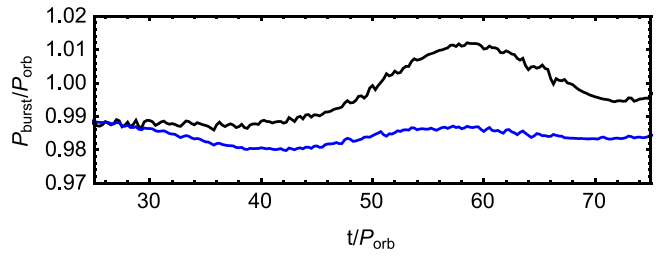

Figure 3. The timescale between the neutron star passing the disk longitude of ascending node (blue) and the disk apastron (black) calculated with Equation (1).

The third row in Figure 1 shows the disk at a time of $t = 36\,P_{\rm orb}$. The disk eccentricity is close to its maximum value of around 0.4. However, the cross section shows that the disk is smaller in the binary orbital plane than at $t = 30\,P_{\rm orb}$ because the disk has apsidally precessed. The accretion is dominated by that from the node crossings and the outbursts occur on a timescale slightly less than $P_{\rm orb}/2$ between $t = 36$–$39\,{\rm P_{orb}}$. During this period of high eccentricity, the average accretion rate onto the neutron star is much higher but the amplitude of these outbursts is relatively low.

At a time of about $40\,P_{\rm orb}$ the accretion again has one main outburst per orbital period but subpeaks can be seen. The fourth row in Figure 1 shows the disk at this time. The argument of periapsis is 81° and the size of the disk in the cross section of the binary orbital plane is small. The amplitude of the outbursts grows in time for a few orbital periods. At a time of about $t = 45\,P_{\rm orb}$, the argument of periapsis passes through 90°. At this time we clearly see the three peaks per orbital period. The middle and largest amplitude peak is due to the disk eccentricity while the subpeaks on each side are where the neutron star passes the nodes of the disk. The delay between the disk eccentricity peak and the following node peak is particularly evident at 41–45 $P_{\rm orb}$ in Figure 4.

The bottom row in Figure 1 shows the disk at a time of $t = 50\,P_{\rm orb}$ where the disk eccentricity has significantly decreased. The eccentricity at this time is similar to that at $t = 30\,P_{\rm orb}$; however, the accretion rate shows two outbursts per orbital period compared to one at $t = 30\,P_{\rm orb}$. The cross section in the binary orbital plane shows that the disk is fairly symmetric in this plane. The outbursts occur when the neutron star passes close to the two nodes of the disk on each orbital period and the outbursts are of similar magnitudes. We note that in the right-hand panels of Figure 1 we can see that there is a circumbinary disk forming around the binary (see also Franchini & Martin 2019).

At a time of around $t = 72\,P_{\rm orb}$ the disk reaches the peak eccentricity of the second KL cycle (see Figure 2). The argument of periapsis passes through −90° and we again see evidence of three outbursts per orbital period with the largest magnitude outburst coming from the disk apastron crossing. The material captured at the disk apastron dominates and we do not get the nonperiodic behavior again. We have not included accretion into the Be star disk from the star and so the inclination of the disk decays over time. However, if there was a source of high inclination material being added to the disk the KL disk oscillations may be more long lived. This has been seen in the case of a circumbinary disk that feeds the formation of circumstellar disks at high inclination (Smallwood et al. 2021). Thus, the nonperiodic outburst phase may be able to repeat in time and the outbursts would periodically show these frequency changes (see also Suffak et al. 2022).

2.4. Application to RX J0529.8–6556

The orbital period of the binary that we have considered in the simulation is relatively short. However, we expect the physics to be the same for a system with longer orbital period provided that the disk is sufficiently large to be tidally truncated (e.g., Martin et al. 2011). We have also run a simulation with a small binary eccentricity of 0.1 and we find very similar behavior. Bearing these in mind, we can compare our model to the observed light curve for RX J0529.8–6556. The accretion rate in Figure 4 between a time of about 37–48 $P_{\rm orb}$ has a similar shape to the light curve observed in Treiber et al. (2021). Initially the outbursts occur on a short timescale that is about $P_{\rm orb}/2$ and these outbursts have a relatively small amplitude. The time between outbursts increases over time as does the amplitude of the outbursts. While we have not tried to tune our model parameters to get the closest possible fit, we can make a prediction about the orbital period of the system. The short period outbursts at the start ($t \approx 37\,P_{\rm orb}$) are on a timescale of $0.98\,P_{\rm orb}/2$ (see the blue line in Figure 3). In the observed light curve, the outbursts are every 149 day and so we suggest that the orbital period of this system could be about 305 days.

We also ran a simulation with the same initial disk inclination, i.e., $i = 50°$, but with a binary eccentricity of 0.34. While the disk has low eccentricity, the dominant effect is the binary eccentricity and outbursts occur close to the binary periastron passage on the orbital period. When the disk becomes eccentric because of the KL effect, the outbursts are dominated by the disk eccentricity and these occur once per orbital period when the neutron star passes the disk apastron.

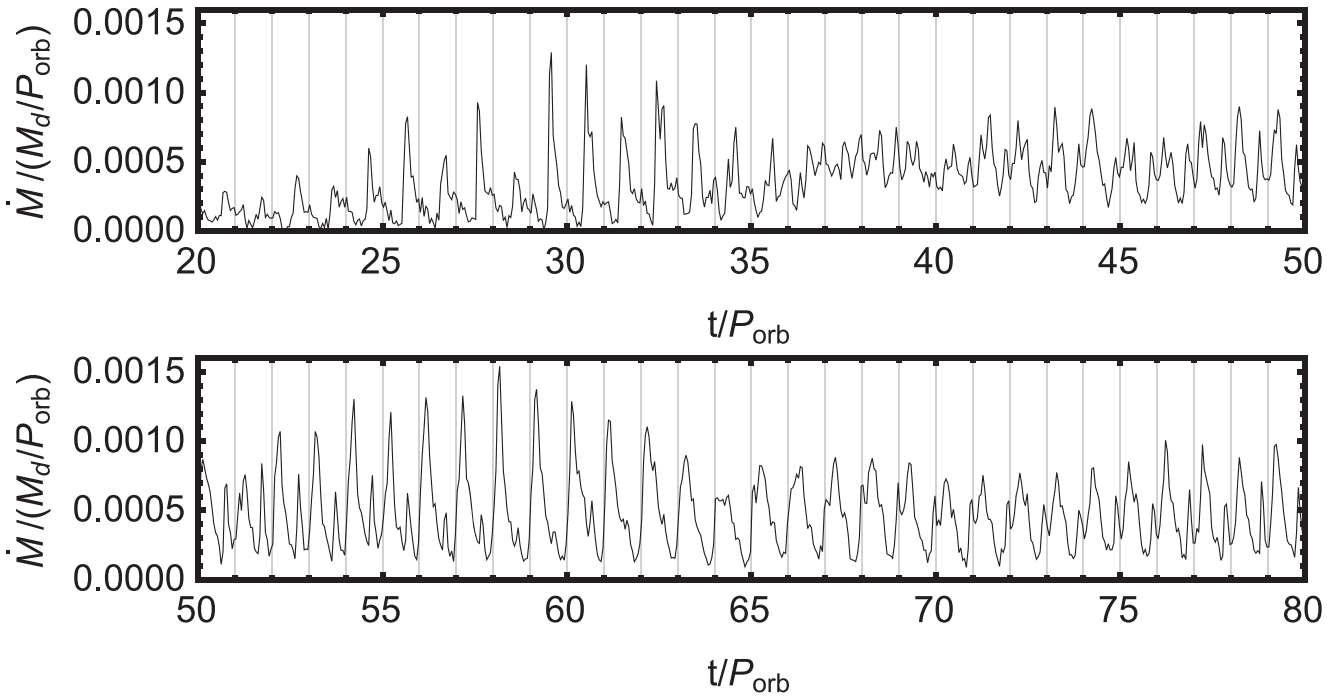

Figure 4. Accretion rate onto the neutron star as a function of time.

The transition between these two regimes is quick and we do not observe significant changes to the outburst period aside from at these transitions.

3. Conclusions

Periodic type I outbursts may be driven by either a moderate binary orbital eccentricity or disk eccentricity in a circular orbit binary. We have shown that nonperiodic outbursts may be temporarily driven in a binary that is close to circular with an inclination such that the disk is mildly unstable to KL disk oscillations. The inclined and eccentric disk transfers material at up to three locations during each orbital period: the two nodes of the disk and the disk apastron. The relative magnitude of each depends upon the argument of periapsis of the disk. The timing of each outburst depends upon the rate of the nodal and apsidal precessions that go in opposite directions. The rapid nodal precession during a KL cycle can lead to rapid changes to the outburst period.

We thank an anonymous referee for useful comments. Computer support was provided by UNLVs National Supercomputing Center. R.G.M. acknowledges support from NASA through grant 80NSSC21K0395. A.F. acknowledges financial support provided under the European Union's H2020 ERC Consolidator Grant "Binary Massive black hole Astrophysics" (B Massive, grant Agreement: 818691). We acknowledge the use of SPLASH (Price 2007) for the rendering of Figure 1.

ORCID iDs

Rebecca G. Martin https://orcid.org/0000-0003-2401-7168
Alessia Franchini https://orcid.org/0000-0002-8400-0969

References

Bate, M. R., Bonnell, I. A., & Price, N. M. 1995, MNRAS, 277, 362
Caceres, G. A., Feigelson, E. D., Jogesh Babu, G., et al. 2019, AJ, 158, 58
Carciofi, A. C., Bjorkman, J. E., Otero, S. A., et al. 2012, ApJL, 744, L15
Cheng, Z. Q., Shao, Y., & Li, X. D. 2014, ApJ, 786, 128
Feigelson, E. D., Babu, G. J., & Caceres, G. A. 2018, FrP, 6, 80
Franchini, A., & Martin, R. G. 2019, ApJL, 881, L32
Franchini, A., Martin, R. G., & Lubow, S. H. 2019, MNRAS, 485, 315
Fu, W., Lubow, S. H., & Martin, R. G. 2015a, ApJ, 807, 75
Fu, W., Lubow, S. H., & Martin, R. G. 2015b, ApJ, 813, 105
Haberl, F., & Sturm, R. 2016, A&A, 586, A81
Hanuschik, R. W. 1996, A&A, 308, 170
Jones, C. E., Sigut, T. A. A., & Porter, J. M. 2008, MNRAS, 386, 1922
King, A. R., Pringle, J. E., & Livio, M. 2007, MNRAS, 376, 1740
Kozai, Y. 1962, AJ, 67, 591
Lee, U., Osaki, Y., & Saio, H. 1991, MNRAS, 250, 432
Lidov, M. L. 1962, P&SS, 9, 719
Lodato, G., & Price, D. J. 2010, MNRAS, 405, 1212
Lubow, S. H. 1991a, ApJ, 381, 259
Lubow, S. H. 1991b, ApJ, 381, 268
Lubow, S. H. 1992, ApJ, 401, 317
Lubow, S. H., Martin, R. G., & Nixon, C. 2015, ApJ, 800, 96
Lubow, S. H., & Ogilvie, G. I. 2017, MNRAS, 469, 4292
Martin, R. G., & Franchini, A. 2019, MNRAS, 489, 1797
Martin, R. G., Nixon, C., Armitage, P. J., Lubow, S. H., & Price, D. J. 2014a, ApJL, 790, L34
Martin, R. G., Nixon, C., Lubow, S. H., et al. 2014b, ApJL, 792, L33
Martin, R. G., Nixon, C. J., Pringle, J. E., & Livio, M. 2019, NewA, 70, 7
Martin, R. G., Pringle, J. E., Tout, C. A., & Lubow, S. H. 2011, MNRAS, 416, 2827
Miranda, R., & Lai, D. 2015, MNRAS, 452, 2396
Negueruela, I., Okazaki, A. T., Fabregat, J., et al. 2001, A&A, 369, 117
Okazaki, A. T. 2007, in ASP Conf. Ser., 367, Massive Stars in Interactive Binaries, ed. N. St. Louis & A. F. J. Moffat (San Francisco, CA: ASP), 485
Okazaki, A. T., Hayasaki, K., & Moritani, Y. 2013, PASJ, 65, 41
Okazaki, A. T., & Negueruela, I. 2001, A&A, 377, 161
Pfahl, E., Rappaport, S., Podsiadlowski, P., & Spruit, H. 2002, ApJ, 574, 364
Porter, J. M. 1996, MNRAS, 280, L31
Price, D. J. 2007, Pasa, 24, 159
Price, D. J., & Federrath, C. 2010, MNRAS, 406, 1659
Price, D. J., Wurster, J., Tricco, T. S., et al. 2018, PASA, 35, e031
Pringle, J. E. 1991, MNRAS, 248, 754
Rajoelimanana, A. F., Charles, P. A., & Udalski, A. 2011, MNRAS, 413, 1600
Reig, P. 2007, MNRAS, 377, 867
Reig, P. 2011, Ap&SS, 332, 1
Rímulo, L. R., Carciofi, A. C., Vieira, R. G., et al. 2018, MNRAS, 476, 3555
Shakura, N. I., & Sunyaev, R. A. 1973, A&A, 24, 337

Slettebak, A. 1982, ApJs, 50, 55
Smallwood, J. L., Martin, R. G., & Lubow, S. H. 2021, ApJL, 907, L14
Suffak, M., Jones, C. E., & Carciofi, A. C. 2022, MNRAS, 509, 931
Treiber, H., Vasilopoulos, G., Bailyn, C. D., et al. 2021, MNRAS, 503, 6187
Whitehurst, R. 1988, MNRAS, 232, 35
Zanazzi, J. J., & Lai, D. 2017, MNRAS, 467, 1957